SOLAR-SYSTEM DYNAMICS AND TESTS OF GENERAL RELATIVITY WITH PLANETARY LASER RANGING

J. F. Chandler (1), M. R. Pearlman (1), R. D. Reasenberg (1), J. J. Degnan (2)
(1) SAO, Harvard-Smithsonian Center for Astrophysics. (2) Sigma Space Corporation
jchandler@cfa.harvard.edu

Abstract

The solar system is the classical laboratory for testing the laws of gravity. Many of the most important tests of general relativity have been made using solar-system bodies. These include tests based on the advance of the perihelion of Mercury, the deflection of starlight passing near the Sun, the Shapiro time delay to the Viking landers, the frequency shift of signals to the Cassini spacecraft, and the (lack of) violation of the equivalence principle manifest by the motion of the Moon (Nordtvedt effect). Planetary Laser Ranging (PLR) promises to open up a new era of tests by yielding a major advance in the measurement of the distance between Earth and a planet. We present the results of a series of covariance studies that include the massive SAO set of solar-system data augmented by PLR pseudo-data under a variety of assumptions. In particular, we consider PLR to Mars and its contribution to a time-delay test, to the measurement of the relativistic advance of planetary perihelia, and to the bound on the time-variation of the strength of the gravitational interaction (G), as measured in a system of units defined by atomic processes (e.g., using atomic time). We find a time-delay test approaching a part in 10^7 in a multi-year experiment.

I. Introduction

Planetary laser ranging (PLR) offers three types of scientific output: solar-system dynamics, tests of general relativity, and studies of the target planet. Any solar-system object with a solid surface and a transparent atmosphere would be a suitable platform for a PLR system, but some objects are more accessible than others. There would of course be considerable interest in improved ranging to Mercury for all three categories of science, but we recognize that an easier target might be a better place to start. In this paper, we consider the case of a single PLR system on Mars although we note advantages in placing two or more systems to help in separating individual effects that would fall within reach of the dramatically improved sensitivity of PLR.

In this section, we describe some of the scientific uses of PLR to set the stage for a more detailed discussion of some of them. Since this is a preliminary survey, we allow for different levels of accuracy for the ranging normal points: we assume the single-day measurement uncertainties would be between 1 mm and 100 mm.

Solar System Dynamics. A precise measure of the Earth-Mars distance, measured between their centers of mass and taken over an extended period, would support the better determination of numerous parameters of the solar-system model. Among these would be the orbital elements of both Earth and Mars, several planetary masses, the masses of many asteroids, and, indirectly, the orbital elements of some of the outer planets (Jupiter, Saturn, and possibly Uranus). These model improvements would be of interest, not only for their own sakes, but also as a necessary step toward testing general relativity.

Relativity Tests. The Shapiro time delay has been measured by the Viking Mission to 1 part in 10^3 (Reasenberg et al. 1979) based on ranging to the landers with a few meters of

uncertainty. The solar corona corrupted the most valuable data, forcing the experiment to rely on data less sensitive to the effect. Note that the same relativistic space-time curvature which gives rise to the Shapiro delay also produces related effects for electromagnetic signals passing near a massive body, such as the frequency shift related to a changing impact parameter and the deflection. For example, the deflection of radio waves has been measured to 2 parts in 10^4 (Shapiro et al. 2004) using very-long-baseline interferometry. Also, the delay rate or frequency shift has been measured by the Cassini Mission to 1 part in 10^5 (Bertotti et al. 2003).

With PLR, there could be an improvement of at least two orders of magnitude beyond the Cassini result. This is sufficient to see the term proportional to the square of the solar mass, a spectacular qualitative improvement, with possible implications for discriminating among theories. To achieve such accuracy in the delay test, data would be needed over an extended period, not just during a short span around superior conjunction (when the effect is at a maximum). As noted above, the solar-system model as a whole needs to be improved concurrently with the relativity test. We present the results of sensitivity studies of the delay test in section II.

One hears about the relativistic advance of the perihelion of Mercury (nominally 43 seconds of arc per century) because it is large and historically important in the confirmation of general relativity. The effect for Mars is smaller by a factor of about 14 (measured in distance per unit time), and the lower eccentricity of the orbit (9.3% vs. 20.5%) makes the effect correspondingly more difficult to observe. However, the measurements of Mercury have been limited to planetary radar with an uncertainty typically around 100 m, and corrupted by still larger topography. The range of topographic relief on a terrestrial planet is on the order of 10 km, and, although the large-scale variations can be modeled and removed after observing the planet through many apparitions, there are local features of up to about 1 km that can be removed only by the use of the rare "closure points" where the same spot on the surface is observed at widely separated times. Even the closure points provide only partial cancellation of topographic noise because of the imperfect overlap and evolving radar technology that yields different footprints at different epochs.

In contrast, repeated ranging measurements to a fixed point on the surface require only the planetocentric position of the point in question and a model of planet rotation for reducing the measured distances to center-of-mass distances. For sufficiently precise data, the former might need to be time-dependent and the latter, very detailed. For Mars, the Viking and Pathfinder landers provided ranging uncertainties of 5-10 m, about two orders of magnitude better than Mercury radar, but mm-level PLR measurements of Mars would be over five orders of magnitude better than Mercury radar, and the perihelion advance would, in principle, be measured better by more than three orders of magnitude. Nonetheless, the time span of Mercury radar data is measured in decades, encompassing many perihelia. Obtaining a comparable time span for PLR may be difficult. Our sensitivity studies have shown that even five years of PLR measurements for Mars would just barely begin to separate out the perihelion advance from the other observable effects that can mask it. Note that a secular effect, like the perihelion advance, bestows a particular advantage upon long-term observations because the expected signature grows with time.

There has long been a question of the possibility that the strength of the gravitational interaction (G), as measured in a system of units defined by atomic processes (e.g., using atomic time), may be varying. It was discussed by Dirac (1937) in connection with the Large

Numbers Hypothesis, but it has many modern incarnations, including those in string theory. The effect of Ġ, as it is known, is to advance a planet along its orbit by an extra distance that grows quadratically with time. For the Earth-Mars distance, the observations go back decades, but the extreme accuracy of PLR data could allow a significant improvement in the uncertainty of the Ġ estimate based on a few years of data taking. We examine this effect in more detail in section II.

If, as expected, Mars is a "proper rotator," then its rotation period (after accounting for geophysical effects) is constant in proper time. Because the Mars orbit is eccentric (9.3%), the rotation period (as measured in the barycentric frame) will change by about 1 part in 10^9 over a Martian year. This was nearly detectable with Viking data. It would be well observed with PLR data and would be the first observation of the proper rotation of a planet. The principal challenge would be to separate the relativistic effect from the seasonal effects due to mass and angular-momentum transfers between planet and atmosphere. Fortunately, proper rotation has already been observed in binary pulsars (Smarr and Blandford 1976). Thus, we are free to assume proper rotation in the case of Mars and to use the observations to study the Mars geophysical effects.

Studies of Mars. At the mm level, a wide array of Mars-specific physical effects will be manifest in the data. A detailed analysis of such effects is beyond the scope of this paper, but we mention some of them here for background. Variations in rotation rate (UT) will be due to the deposit and release of atmospheric material at the poles as well as global wind patterns. Similarly, there will be wobble terms due to related processes. These atmospheric effects fall under the heading of *weather* and thus will vary at all time scales. Solid body tides should be visible, and it may be possible to model the elastic properties of the body. By looking at the precession and nutation of Mars, it should be possible to bound or measure the non-elastic (i.e., liquid) behavior of the core. Through the reflex motion of Mars around the Mars-satellite center of mass, we might obtain a measure of the masses of Phobos and Deimos, the two satellites of Mars. These masses might also be determined through the Mars nutation they induce. Finally, we note that separating the numerous effects would require the use of more than one PLR system on the surface of Mars. Further, the separation of the myriad effects, many of which have well defined temporal signatures, would require an extended observing period. In return for this effort, we would learn about many aspects of the planet.

II. Design of Sensitivity Studies

In this section, we discuss a series of studies designed to illustrate the results that might be obtained with a PLR transponder on Mars. In order to provide some realism, these studies combined our current solar-system data set with the hypothetical PLR data in a simultaneous covariance analysis. Table 1 shows a summary of the parameters in our model of the solar system. Since the 1548-parameter model already includes the orientation of Mars (necessary for the Viking and Pathfinder lander range data), we need only three additional parameters (coordinates of the PLR transponder) to handle the hypothetical PLR data. The parameters shown in the table relate to dynamical and physical properties of the observed bodies, and are thus of some intrinsic interest, but the present analysis focuses on others (shown in Table 3) that characterize possible violations of general relativity.

Table 1. Solar-System Analysis Model

Parameter Type	Number
Masses	19
Asteroid class densities	5
Moon mass distribution	9
Sun mass distribution	1
Orbital elements	43
Earth-Moon tides	3
Earth orientation	364
Moon orientation	6
Mars orientation	9
Interplanetary plasma density	1
Station coordinates	33
Target coordinates (Moon)	12
Target coordinates (Mars)	9
Mercury topography	566
Venus topography	444
Measurement biases	24

Although one can infer the existence, and even the dynamical properties, of other planets through their perturbations of the orbits of Mars and the Earth as seen via precise Earth-Mars ranging, the real task at hand is to characterize the scientific gains due to PLR in the context of knowledge already available. Thus, our current data set provides the backdrop for studying the uses of PLR. Table 2 shows the types and numbers of the solar-system data used in our studies. For the purposes of this study, we are not assuming any additional data of these types will be acquired. We believe this assumption does not significantly affect our conclusions.

Table 2. Supporting Data Sets

Type	Number	Range Uncertainty	Time Span
Mariner 9 normal points	185	30 m - 300 m	1971-1972
Viking lander delays	1280	2 m - 20 m	1976-1982
Pathfinder delays	90	10 m - 20 m	1997-1997
Outer planet normal points	6	3 km - 50 km	1973-1979
Mercury radar delays	8054	30 m - 150 m	1969-1997
Venus radar delays	5674	20 m - 750 m	1969-1982
LLR normal points	13538	3 cm - 30 cm	1969-2001

The goals of these studies include an exploration of the dependence of scientific output on three factors: the accuracy of the ranging data (assumed to be from 1 to 100 mm), the longevity of the transponder, and the Sun avoidance angle. The first of these would give a simple scale factor were we not using a fixed set of other data (Table 2) to condition the analysis. The second factor, experiment duration, is likewise complicated by the other data;

in their absence, the results would show a power-law dependence on duration. The third factor, Sun avoidance, is crucial to the time delay experiment, since the effect is sharply peaked at superior conjunction, when both the ground-based telescope and the PLR transponder must point nearly at the Sun. Figure 1 shows the time dependence of the Shapiro delay through two superior conjunctions of Mars. In Section IV, we discuss some of the issues in setting the Sun avoidance angle. In this context, we note that duration is not the only important timing consideration, since a one-year mission in 2004 or 2006 would cover a superior conjunction, while a one-year mission in 2005 or 2007 would not. In nearly all of the studies, we began the observations on 2004 Mar 18, six months before the imminent superior conjunction.
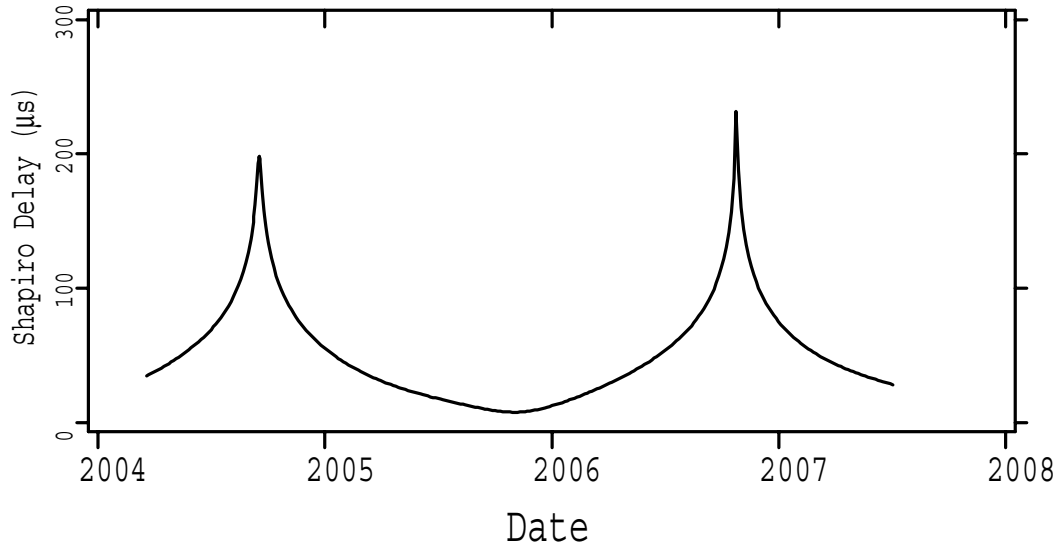
Figure 1: Contribution of the Shapiro effect to the Earth-Mars-Earth delay

Each covariance study was done in the same manner. We assumed a PLR transponder near, but not on, the Mars equator (specifically, at 11° N and 99° W). The longitude does not matter, and the latitude scarcely matters because we took dummy data as if both Mars and the Earth were transparent. Also, we assumed only one observatory taking data (the McDonald Laser Ranging Station). The normal observing schedule was one observation every four days, but we assumed a special effort would be made near superior conjunction, with daily observations during the month centered on each superior conjunction (the first being 2004 Sep 15). This schedule was subject to the Sun avoidance criterion, but all allowed observations on the schedule were assumed to be made successfully and with the same measurement uncertainty between the designated start and stop dates. Each study was performed three times, once with each of the three chosen round-trip range uncertainties: 1 mm, 10 mm, and 100 mm. We also covered a broad range of duration (up to 5 years) and Sun avoidance angle (0.5 to 15°). In this study, we defined the avoidance angle as the minimum angle between the limb of the Sun and the target, as seen from one of the observing stations. For simplicity, we applied the Sun avoidance criterion only to the Earth observatory. (At superior conjunction, the relative Mars-Sun-Earth distances are always about the same, and the Earth-based criterion therefore maps into a consistent, though different, Mars-based criterion.) It is important to note that the Sun-Earth angle as seen on Mars near conjunction is about 2/3 of the Sun-Mars angle as seen on Earth, and therefore the Sun avoidance is inherently a more difficult problem for the PLR transponder than for the Earth observatory.

III. Results of Sensitivity Studies

Figures 2-4 display the results of our studies. They show the dependence of scientific output on the three design variables: measurement uncertainty, experiment duration, and Sun avoidance criterion. In broad outline, the first two variables behave in much the same way for all of the tests. At short duration, the predictions of our existing solar-system model are extrapolations because we are not assuming any extension of our existing data set. Thus, the PLR data cannot contribute at full strength to the relativity tests at first. However, when the geometry becomes favorable, the parameter uncertainties associated with the three levels of measurement uncertainty separate and gradually approach saturation, where the PLR contribution dominates the test, and the sensitivity simply scales with measurement uncertainty.

As can be seen in Figure 2, the time delay test rapidly approaches saturation after the first superior conjunction (six months into the experiment). In contrast, the $\dot{G}$ test shown in Figure 3 is nowhere near saturation even after five years. The perihelion test (not shown) is comparable to the $\dot{G}$ test, in terms of both the maximum improvement (about a factor of ten) over the five-year duration and the spread (about a factor of three) between 1 mm and 100 mm results. It is clear that the payoff for the time-delay test is optimum as long as the experiment covers at least one conjunction and a sufficient time before or after to refine the solar-system model. On the other hand, the $\dot{G}$ and perihelion tests benefit from a PLR experiment that lasts as long as possible. This contrasting behavior stems from the difference between stationary and secular effects. Despite this contrast, we compare the payoffs for all three tests after a uniform two years in Table 3.
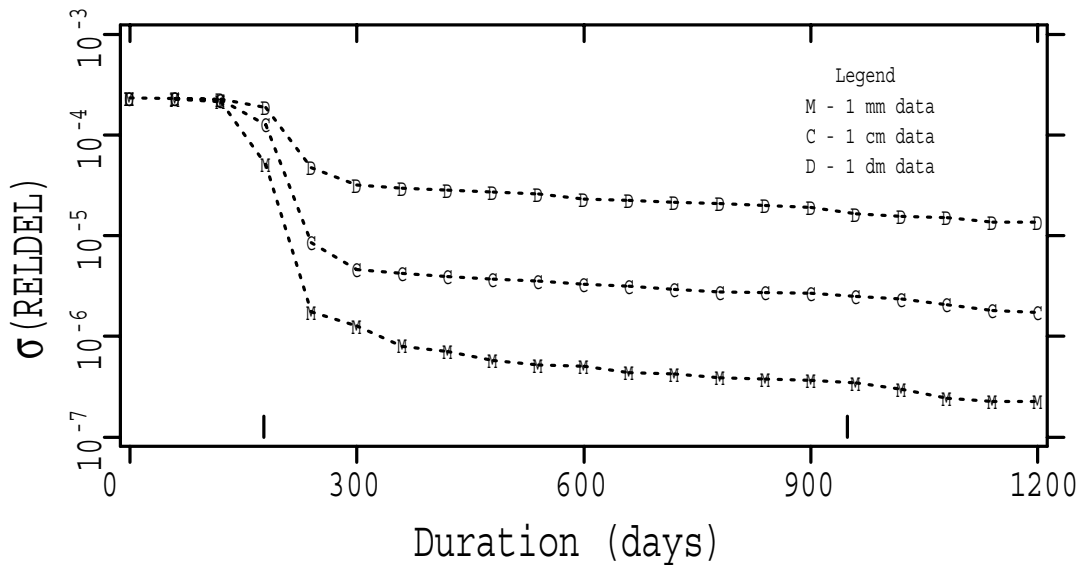
Figure 2: Dependence on duration of the time-delay test, using 5° Sun avoidance. The dramatic reduction in σ(RELDEL) about six months corresponds to the first superior conjunction (marked). The reduction at the similarly marked second superior conjunction is the expected √2 change.
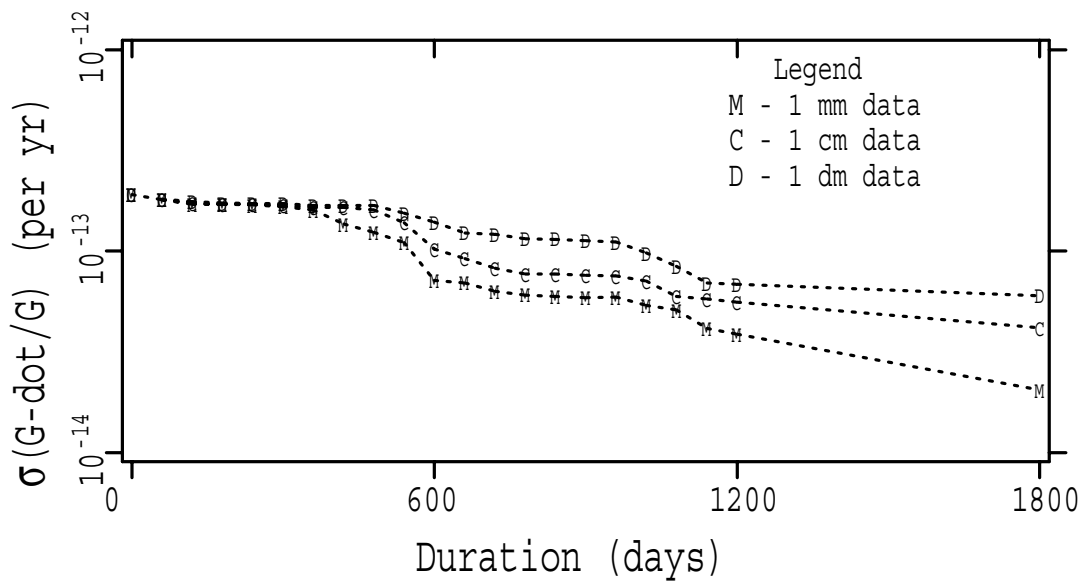
Figure 3: Dependence on duration of the Ġ test, using 5° Sun avoidance.

Table 3. Scientific payoffs after two years with 15° Sun avoidance. Payoff is here defined as the ratio of starting standard error to final standard error of the stated parameter. RELDEL and RELFCT are model coefficients for the time delay and the relativistic motion (including perihelion advance), respectively.

	Measurement Uncertainty		
Test	100 mm	10 mm	1 mm
Ġ	1.6	2.4	3.0
RELDEL	2.4	10.2	48.6
RELFCT	2.7	6.5	8.7
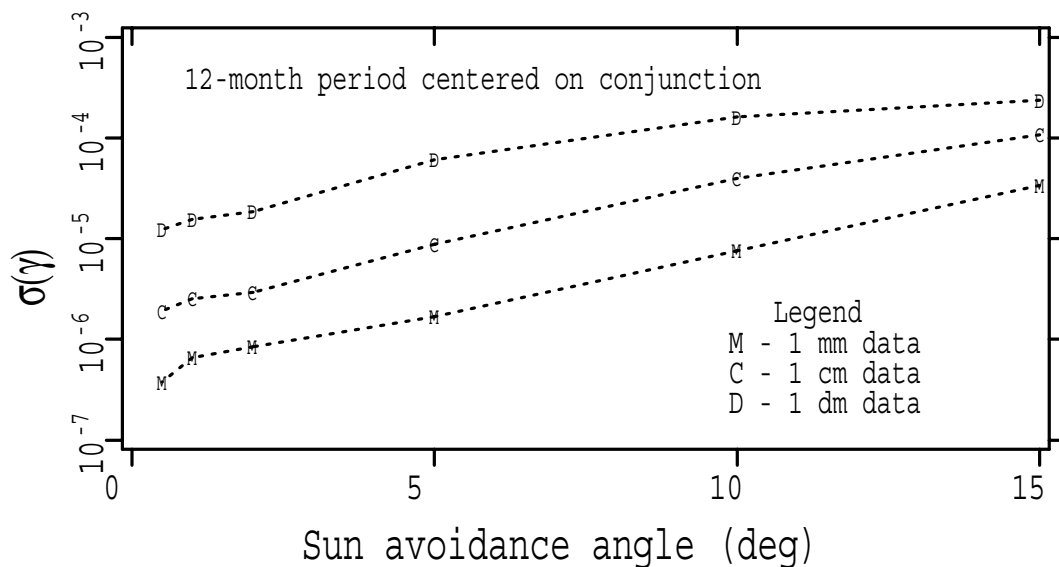
Figure 4: Dependence of the time-delay test on Sun avoidance, using 12 months of data. The closest approach in this apparition (2004) is 0.75°. For avoidance angles of 5° or more, the entire month around conjunction is blocked.

Figure 4 shows the dependence on Sun avoidance angle of the sensitivity of the time-delay test in a one-year experiment. For angles of 5° or more, the entire one-month period of daily observations is disallowed. Other factors, such as the orbital eccentricity, contribute to the complexity of detail in the figure. The striking result is that the test can be strengthened by as much as two orders of magnitude for 1 mm data by narrowing the Sun avoidance angle from 15° to 0.75°. This contrast provides the motivation for observing as close to the Sun as possible. As expected, there is little dependence on avoidance angle in the other tests.

IV. Working Close to the Sun

Measurement of the Shapiro delay requires operation of the transponder over propagation paths which pass very close to the solar disk. For such observations, one must be concerned about possible optical damage to the detector, excessive solar heating of the instrument, and excessive background noise due to solar scattering within the instrument that might obscure the transponder signal. Accurate navigation and attitude information plus Sun avoidance hardware/software are clearly baseline requirements for such a mission.
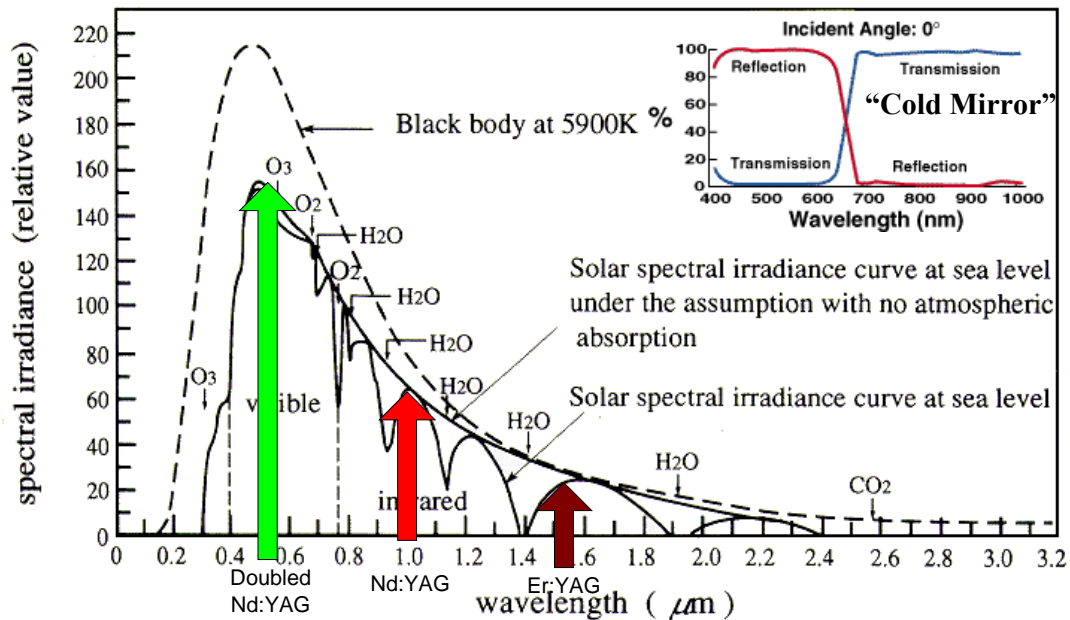
Figure 5: Exo-Atmospheric solar spectral irradiance (dashed curve) and at sea level with and without atmospheric absorbers. Also shown are three popular visible and near-IR laser wavelengths for which short pulse microchip lasers exist – Doubled Nd:YAG (532 nm), Nd:YAG (1064 nm), and Er:YAG (1550 nm). The inset shows the typical transmission and reflection properties of a "cold mirror" suitable for a laser with λ > 700 nm.

One approach to minimize the solar problem is to operate at a laser wavelength with good atmospheric transmission and well off the peak of the solar spectrum. Figure 5 displays several items pertinent to this issue:

- The exo-atmospheric solar spectral irradiance approximates that of a black body at 5900° K and has significant output in the UV, visible, and near infrared
- The solar irradiance at sea level due to atmospheric scattering alone

- The solar irradiance at sea level including atmospheric absorbers
- Colored arrows indicating three popular laser wavelengths in the visible and near IR for which short pulse (< 1 ns) microchip lasers and/or high speed detectors exist – Doubled Nd:YAG (532 nm), Nd:YAG (1064 nm), and Er:YAG (1550 nm).
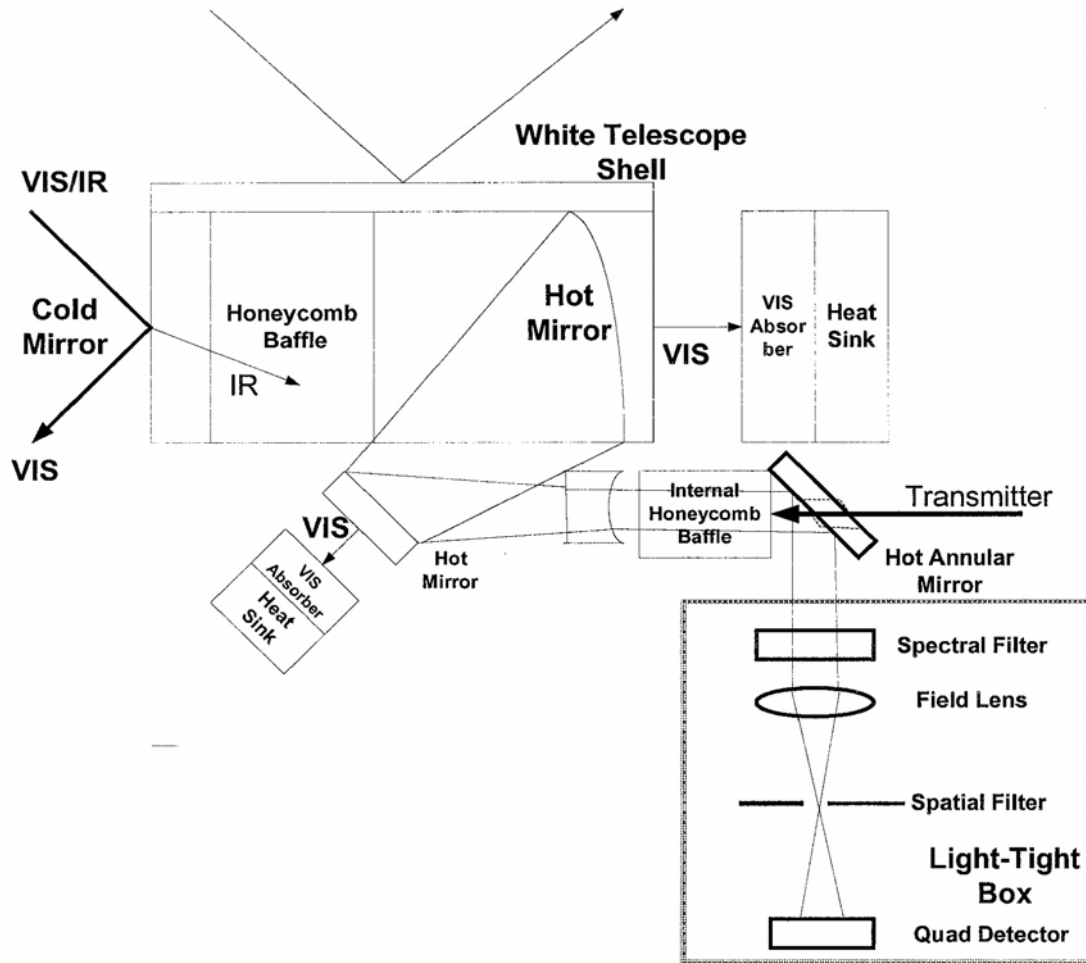
Figure 6: Conceptual design of a transponder for operating along sight lines close to the Sun. In the light-tight box (camera), the detector is placed beyond the focus at the spatial filter to allow the pointing error to be measured (and corrected) over an extended range.

Ideally, one would like to operate the near-Sun transponder well into the infrared where the solar spectral irradiance is greatly diminished and intermittent regions of high atmospheric transmission exist. Unfortunately, the availability of compact, moderate energy, short pulse lasers and/or fast, low noise, high quantum efficiency detectors is problematic beyond 1550 nm. Failing this "ideal" situation, one would at least like to be able to reflect most or all solar irradiance from telescope surfaces and entrance window as in Figure 6. The majority of the solar radiation entering from the upper left-hand corner of the figure is reflected from the outer white shell of the instrument and from the cold mirror entrance window to the telescope. Cold mirrors reflect the shorter, visible wavelengths while transmitting the longer, infrared wavelengths. Their analog, "hot mirrors", do the opposite. In both cases, the center

wavelength separating the regions of reflection and transmission can be tailored to the application by modifying the optical coatings. The inset to Figure 5 also shows the transmission and reflection properties of a typical "cold mirror".

The near infrared solar radiation transmitted by the "cold mirror" entrance window encounters a blackened honeycomb baffle. This second optical barrier defines how closely in angle the transponder can operate to the Sun. In Figure 7, δ_{max} is the acceptance half angle, D is the nominal diameter of the circle which circumscribes the hexagon, and L is the length of the honeycomb tube. To operate within 2° of the Sun, we require that $D/L \leq 0.04$. For near-Sun operation, the interior surface of the honeycomb must be specially treated so that it does not show strong specular reflection at incidence angles approaching $90°$.

Front View

Side View of Individual Cell

$$\delta_{max} = \arctan\left(\frac{D}{L}\right)$$
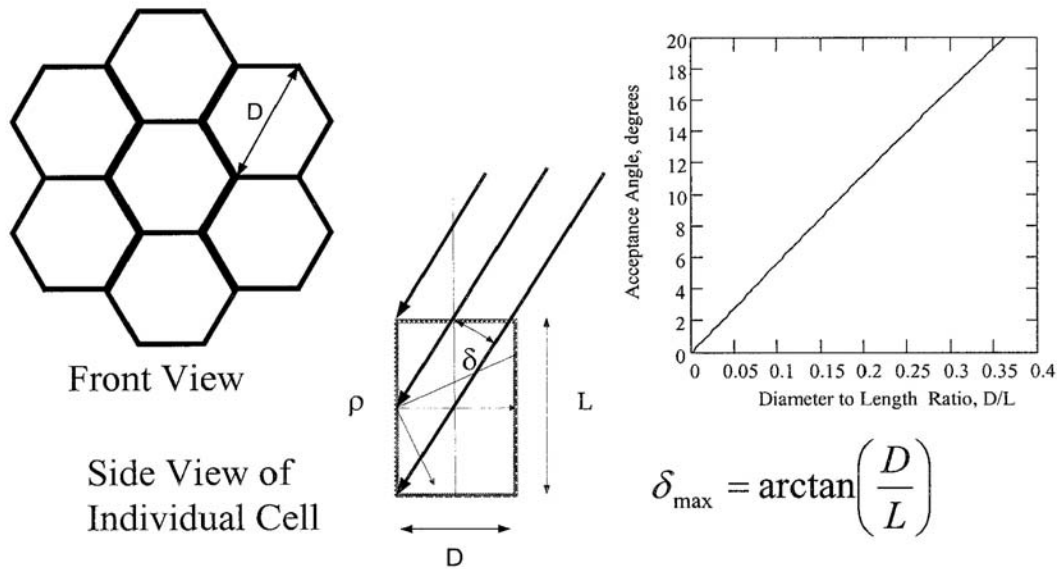
Figure 7: Effect of honeycomb baffle on acceptance half angle for solar radiation.

After being transmitted through the honeycomb baffle, the residual near-IR solar radiation encounters a "hot mirror" primary and a hot mirror fold flat, each of which further filters out the residual short wavelength radiation and transmits it to an absorber, which is thermally coupled to a radiative panel viewing deep space or some other heat dissipation device. After being recollimated by a negative lens and passed through a second (optional) internal honeycomb grid, the transponder signal from the opposite terminal (and any background noise) is reflected by an annular mirror into a light tight receiver box which contains a narrow band spectral filter, a field lens and spatial pinhole, and a quadrant photon-counting detector. The latter outputs an "incoming photon event" to be time-tagged and recorded by the onboard event timer. The photon times of arrival are transmitted back to Earth and combined with similar data at the Earth station to compute a precise time series of Earth-to-spacecraft range and clock offset (Degnan 2002). The timer also records the quadrant that detected the incoming photon, and any imbalance in the quadrant count after many events is used to provide an error signal to the onboard pointing system (Degnan and McGarry 1997).

An interplanetary laser communication system is already being developed for missions to Mars and other targets. The present design includes a Nd:YAG laser at 1064 nm and a requirement of operation at Sun-Earth-target angles as small as $3°$ (Boroson et al 2004).

V. Conclusions

PLR to Mars offers significant potential for improving tests of gravity. These improvements can be realized incrementally, provided that the transponder functions for at least six months, but lifetimes of five years or more would be useful, especially for the tests of secular effects. For measuring the Shapiro delay, it is important for the instruments (both transponder and ground-based telescope) to work as near as possible to the solar limb, but other tests can be performed at much larger Sun avoidance angles. It would be very useful to conduct similar studies with Mercury and with multiple transponders.

References

Bertotti, B., Iess, L., and Tortora, P., "A test of general relativity using radio links with the Cassini spacecraft," Nature, 425, pp. 374-376, 2003.

Boroson, D. M., Biswas, A., and Edwards, B. L., "MLCD: Overview of NASA's Mars Laser Communications Demonstration System," SPIE Vol 5338, Free-Space Laser Communications Technologies XVI, pp. 16-49, Bellingham, WA, 2004.

Degnan, J. J., "Asynchronous Laser Transponders for Precise Interplanetary Ranging and Time Transfer", Journal of Geodynamics (Special Issue on Laser Altimetry), pp. 551-594, November, 2002.

Degnan, John J. and Jan McGarry, "SLR2000: Eyesafe and autonomous satellite laser ranging at kilohertz rates", SPIE Vol 3218, Laser Radar Ranging and Atmospheric Lidar Techniques, pp. 63-77, London, UK, Sept. 24-26, 1997.

Dirac, P. A. M., Nature, 139, p. 323, 1937.

Reasenberg, R. D., Shapiro, I. I., MacNeil, P. E., Goldstein, R. B., Breidenthal, J. C., Brenkle, J. P., Cain, D. L., Kaufman, T. M., Komarek, T. A., and Zygielbaum, A. I., "Viking relativity experiment - Verification of signal retardation by solar gravity," Astrophys J (Lett), 234, pp. L219-L221, 1979.

Shapiro, S. S., Davis, J. L., Lebach, D. E., and Gregory, J. S., "Measurement of the solar gravitational deflection of radio waves using geodetic Very-Long-Baseline Interferometry data, 1979-1999," Phys Rev Lett, 92, p. 121101, 2004.

Smarr, L. L., and Blandford, R., "The binary pulsar: Physical processes, possible companions, and evolutionary histories," Astrophys J, 207, pp. 574-588, 1976.